Journal of Applied Electrochemistry **30**: 939–944, 2000.

Electrochemical hydrogen evolution on polypyrrole from alkaline solutions

MAHMOUD M. SALEH
Chemistry Department, Faculty of Science, Cairo University, Cairo, Egypt

Received 15 February 1999; accepted in revised form 11 October 1999

Key words: conductive polymers, hydrogen, iron, nickel, polypyrrole, porous electrodes

Abstract

Thin films of conductive polypyrrole (PPy) were formed electrochemically from aqueous sulfuric acid. The films showed good electrocatalytic properties towards hydrogen evolution (h.e.r) from alkaline solutions on planar and packed-bed iron electrodes. Current–potential relations were measured at various temperatures and KOH concentrations on Fe, Ni and Fe/PPy planar electrodes. The current was found to be constant during 40 h of operation. SEM micrographs showed no difference in the morphology before and after this period. The activation energy for h.e.r. was found to be 50.2, 58.5 and 33.4 kJ mol^{-1} for Fe, Ni and Fe/PPy planar electrodes, respectively. The results showed that Fe/PPy can be used to produce hydrogen at both ambient and relatively high temperatures $\sim$70 °C. The polypyrrole coating on iron screens was found to reduce the potential required to sustain a specific rate of hydrogen generation and, hence, the energy consumed during the process.

1. Introduction

Water electrolysis is an important means of producing high purity hydrogen for use in applications such as fertilizers, food, chemical and metallurgical industries. These categories include synthesis of ammonia, hydrocracking of petroleum, hydrogenation of fats and oils and as a reducing agent in the metallurgical and semiconductors industries. The process is achieved using proven technology and its fundamental electrochemistry is well-documented [1–3]. The main operating cost of the process is the cost of electricity. Consequently, research and development efforts have been directed towards minimizing ohmic and activation overpotentials through improving cell and electrode designs and the search for electrode material with better electrocatalytic activity [4]. Since electrochemical reactions are essentially surface reactions, their rates can be substantially increased by improving the electrocatalytic activity and/or increasing their surface area.

Conductive polymers such as polypyrrole have shown good electrocatalytic properties towards many electrochemical reactions. Potential applications for polypyrrole include microcircuit transistor devices, electrochromic devices, batteries, ion exchangers, corrosion protection, sensors and electrocatalysis [5–11]. Electrodeposition of polypyrrole layers has been performed from aqueous [12, 13] and nonaqueous media [14, 15]. Mainly inert electrodes such as Pt, Au and GC have been used [16–19]. However, active Fe and Al have also been used and good adhesion of PPy layers on iron and on aluminium electrodes has been reported [20–22]. Beck et al. studied the feasibility of polypyrrole electrodeposition on Al for battery applications [20] and they also electrodeposited the polymer on different metals including Fe [21, 22]. Bloor et al. electrodeposited polypyrrole on mild steel from pyrrole solutions in propylene carbonate [23] and Lacaze et al. showed that strongly adherent PPy films can be obtained from different aqueous solutions on iron [24]. Some authors [20–24] have tested the redox, structural and physical properties of the formed polypyrrole, but no electrochemical applications such as hydrogen evolution reaction was performed on the polymer.

Flow through porous electrodes can also be used to increase the surface area by up to several orders of magnitude on the small cell scale. The theory and applications of these systems have been developed and discussed [25, 26]. Different packing materials for flow-through porous electrodes was used to generate hydrogen from flowing alkaline and acid electrolytes [27, 28].

The aim of this work is to test the feasibility of using polypyrrole coated electrodes for the electrolytic production of hydrogen. Results are presented for planar, as well as packed bed, electrodes.

2. Experimental details

2.1. *Measurements on planar electrodes*

The electrochemical measurements were performed using an EG&G Princeton Applied Research (model 273A) potentiostat/galvanostat controlled by m352

electrochemical analysis software. Three-electrode cells were used. The working electrode was made of either iron, nickel or polypyrrole coated iron (Fe/PPy) electrodes of 1 cm × 1 cm dimensions. The counter electrode was made of a platinum sheet (1 cm × 1 cm) and the reference electrode was SCE. The pyrrole was obtained from Aldrich Chemicals and all other chemicals were analytical grade. The iron and nickel electrodes were polished with emery paper down to 00 grade and then etched in a mixture of sulfuric acid, hydrogen peroxide and water with equal ratio. They were finally degreased by washing with ethyl alcohol and with distilled water. The polypyrrole film was deposited from 0.1 M pyrrole in 0.1 M H_2SO_4 on the iron electrode. The thickness of the polypyrrole film was controlled by measuring the charge passed during the electrodeposition of the film. The generally accepted relationship is that 0.1 C cm^{-2} corresponds to thickness of about 0.70 μm [29]. The thickness of the PPy film used in this work is about 2.5 μm. Current densities are calculated on the basis of the apparent surface area. The surface morphology of the Fe/PPy electrode was examined by scanning electron microscopy (SEM).

2.2. *Measurements on flow-through porous electrodes*

Figure 1 is a schematic illustration of the cell and experimental arrangements of the packed- bed electrode. The screen electrode is held down tightly with a rubber cylinder onto the fritted glass disc to ensure good contact to the platinum wire and to eliminate the possibility of floatation. The upper part of the cell presses onto the rubber cylinder. The electrolytic cell was essentially a cylindrical glass tube which is held upright. The electrolyte was forced from the bottom (entry face) of the cell using a variable speed pump. The working electrode was polarized using a coiled platinum counter electrode placed down stream with respect to the electrolyte flow. Further details for the electrolytic and flow system is given elsewhere [30]. The potentials at both the entry and exit faces of the electrode were measured against two Hg/HgO/1 M KOH reference electrodes (equilibrium potential of 98 mV vs NHE [31]). The potential at the exit face, E_L, is only presented in the present paper for simplicity. The iron screens had a porosity of 0.4, specific surface area of 20 cm^{-1} and the number of the used screens was 6 screens, the thickness of each was 0.5 mm. Each screen was coated individually by polypyrrole as described above, then rinsed in water, dried and packed in the electrode chamber.

3. Results and discussions

3.1. *Results on planar electrodes*

3.1.1. *Current–potential relations*

Figure 2 shows a comparison between the i/E relations for h.e.r. on Fe, Ni and Fe/PPy from 1 M KOH at 30 °C. The polarization required to obtain specific rates of h.e.r on Fe/PPy are lower than for Fe or Ni electrodes. The $i_{o,H}$ value was calculated by extrapolating the Tafel plot to the equilibrium potential of the h.e.r where, $E_H = -0.06$ pH at 30 °C [32]. The values of the $i_{o,H}$ for Fe, Ni and Fe/PPy were calculated to be 5.0×10^{-7}, 4.0×10^{-7} and 5.0×10^{-6} A cm^{-2} in 1 M KOH, respectively. The $i_{o,H}$ for Fe and Ni electrodes are comparable with the values found in the literature [33, 34].

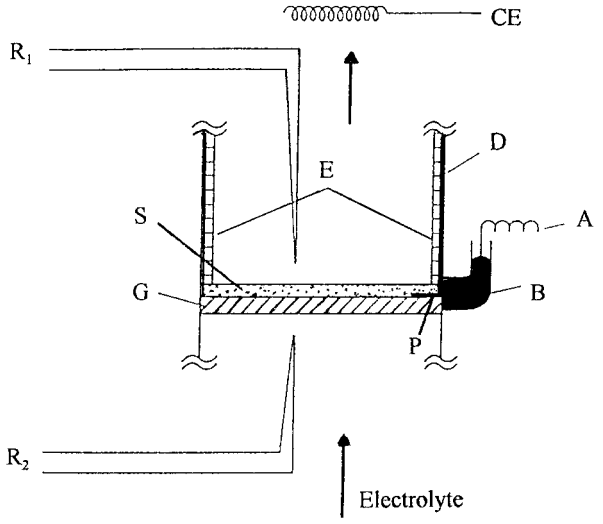

Fig. 1. Schematic diagram of the experimental arrangements for flow-through porous electrodes. Key: (A) connection to the current collector, (B) mercury connection; (D) cell wall, (E) rubber cylinder, (P) platinum current collector, (S) screen electrode (working electrode), (G) fritted glass disc, R1, R2; reference electrodes and (CE) counter electrode.

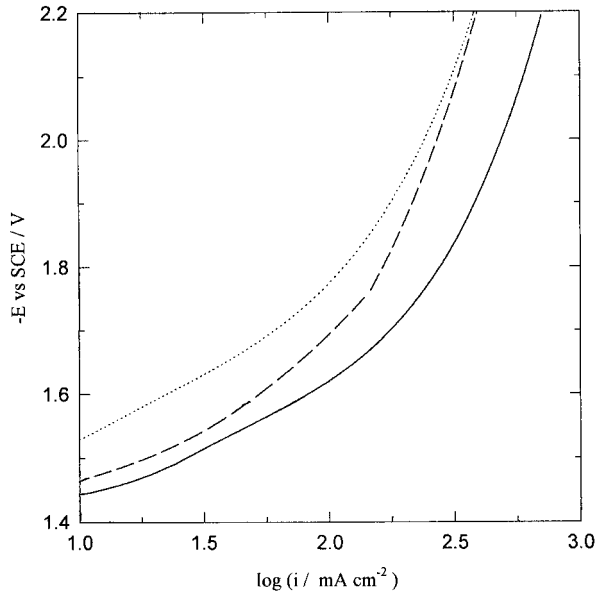

Fig. 2. Comparison of the current-potential relations for h.e.r. at different cathodes from 1 M KOH at 30 °C. Key: (· · · · · ·) Fe, (– – –) Ni and (——) Fe/PPy.

Similar i/E relations were made at 2 and 3 M KOH at 30 °C. Polarizations at different current densities for different cathodes and different KOH concentrations are shown in Table 1. In general, the polarization required to obtain specific current density decreases in the order Fe > Ni > Fe/PPy. The results obtained from Figure 2 and Table 1 imply that the Fe/PPy electrode has enhanced electrocatalytic properties for h.e.r. than that of either Fe or Ni electrodes. This is attributed to both the good electrocatalytic activity of the polypyrrole and to the high surface area of the polymer film due to the roughness of the polymer film (cf. Figure 3).

3.1.2. *Aging effects*

The stability of the Fe/PPy electrode was tested by holding the electrode at a potential of −1.7 V in 2 M KOH for about 40 h at 30 °C. The recorded current–time transient during this period showed a fairly constant current over the duration of the test, which is an indication of the stability of the film. This also points to the good adhesion of the polypyrrole film and to the lack of poising at the polymer surface. The stability of the polymer film was also examined by SEM. Figures 3(a) and (b) show the SEM micrographs of Fe/PPy before and after the above treatment. The morphology of the polypyrrole film was not affected by the evolution of gas bubbles over that period. Visual inspection indicated that no peeling of the film occurred which confirms the stability of the polypyrrole film.

3.1.3. *Effects of temperature*

Since water electrolysis cells operate at relatively high temperatures about 50–70 °C, it is of practical interest to test the stability of the Fe/PPy over this temperature range. Figure 4 shows a comparison between the three electrodes at 70 °C from 2 M KOH. The polarization required to obtain specific rates of hydrogen reaction on Fe/PPy are lower than for Fe or Ni. Similar data were collected at different temperatures for the different cathodes. Table 2 contains the polarization values obtained at different temperatures and current densities

Table 1. Polarizations at different current densities for h.e.r. at different KOH concentrations on different cathodes at 30 °C

Cathode	KOH/M	Cathodic polarizations at different current densities/V		
		1 mA cm^{-2}	2 mA cm^{-2}	2.5 mA cm^{-2}
Fe	1	0.932	1.172	1.522
	2	0.856	1.065	1.355
	3	0.640	0.972	1.151
Ni	1	0.872	1.092	1.472
	2	0.781	0.982	1.323
	3	0.761	0.941	1.201
Fe/Ppy	1	0.842	1.022	1.242
	2	0.801	0.981	1.101
	3	0.780	0.970	1.021

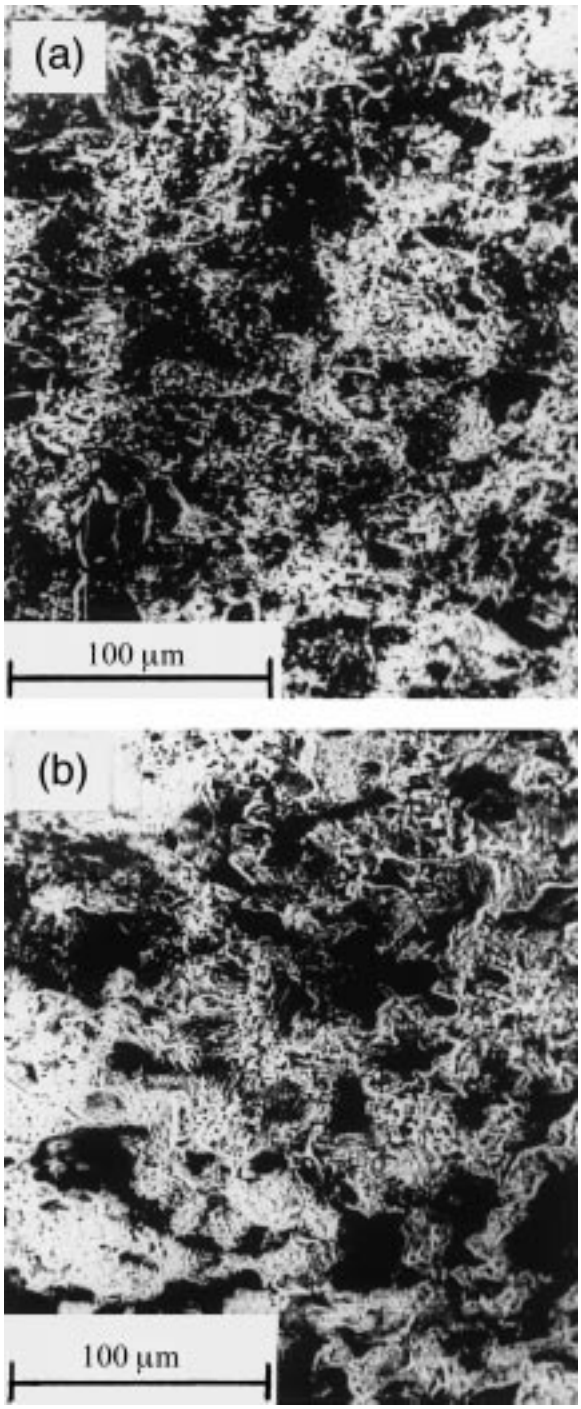

Fig. 3. SEM micrographs of the PPy film (a) before and (b) after using the PPy for 40 h for h.e.r. as in Figure 4.

for the three electrodes. As the temperature increases, the polarization at the same current density decreases. This is attributed to the increase in the rate of charge transfer between the cathode-electrolyte interface. This result also indicates that it is feasible to use the Fe/PPy electrode at high temperatures.

Exchange current densities for the h.e.r for the three electrodes were calculated at different temperatures and used to calculate the activation energy of the h.e.r. on Fe, Ni and Fe/PPy electrodes. Figure 5 shows Arrhenius Plots for the three electrodes. From the slopes, the

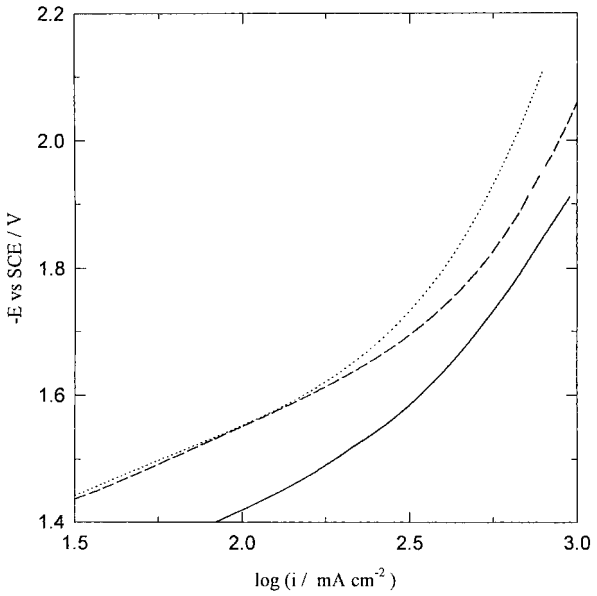

Fig. 4. Comparison of the current-potential relations for h.e.r. at different cathodes at 70 °C from 2 M KOH. Key: (· · · · · ·) Fe, (– – –) Ni and (——) Fe/PPy.

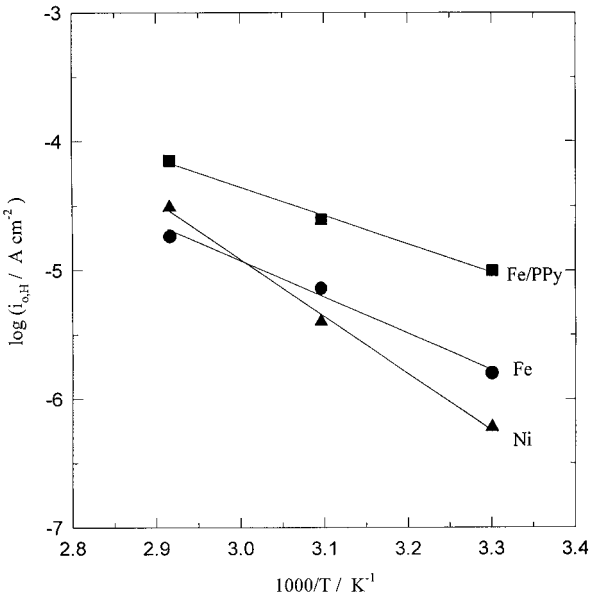

Fig. 5. Arrheniuss Plots for the h.e.r. from 2 M KOH at different electrodes. Key: (●) Fe, (▲) Ni and (■) Fe/PPy.

activation energies were found to be 50.2, 58.5 and 33.4 kJ mol^{-1} for Fe, Ni and Fe/PPy electrodes, respectively. The values of the activation energies for Fe and Ni electrodes are comparable with the values reported in the literatures [33, 34]. The results showed that h.e.r. on PPy is more facile than on Fe or Ni electrodes.

3.2. *Results for the packed-bed*

3.2.1. *Current–potential relations*

Using the porous electrode in the flow regime helps to sweep the hydrogen gas bubbles out of the porous matrix which results in considerable decrease in the polarization of the porous electrode. Furthermore, the evolution of gas bubbles results in a nonuniform distribution of the current and potential inside the porous electrode [35]. A dual benefit can be obtained in coating the iron screens with polypyrrole. One is the high surface area of the small sized porous electrode and the other is the enhanced electrocatalytic activity of the polypyrrole (see the planar electrode section). Figure 6 shows the effects of coating iron screens with polypyrrole on the current-potential relations from an electrolyte of 1 M KOH at 30 °C and at flow rate of 1.0 cm s^{-1}. Coating the electrode with polypyrrole results in considerable decrease in the potential required to maintain a specific rate of hydrogen gas generation.

Table 2. Polarizations at different current densities for h.e.r. at different temperatures on different cathodes from 2 M KOH

Cathode	t/°C	Cathodic polarizations at different current densities/V		
		1 mA cm^{-2}	2 mA cm^{-2}	2.5 mA cm^{-2}
Fe	30	0.856	1.065	1.355
	50	0.684	0.944	1.172
	70	0.630	0.830	0.990
Ni	30	0.781	0.982	1.323
	50	0.663	0.853	1.071
	70	0.590	0.830	0.960
Fe/Ppy	30	0.801	0.981	1.101
	50	0.731	0.923	1.050
	70	0.470	0.690	0.850

3.2.2. *Energy saving*

Coating of the iron screen electrode with the polypyrrole resulted in appreciable decrease in potential which correspond to reduction of the energy consumption at

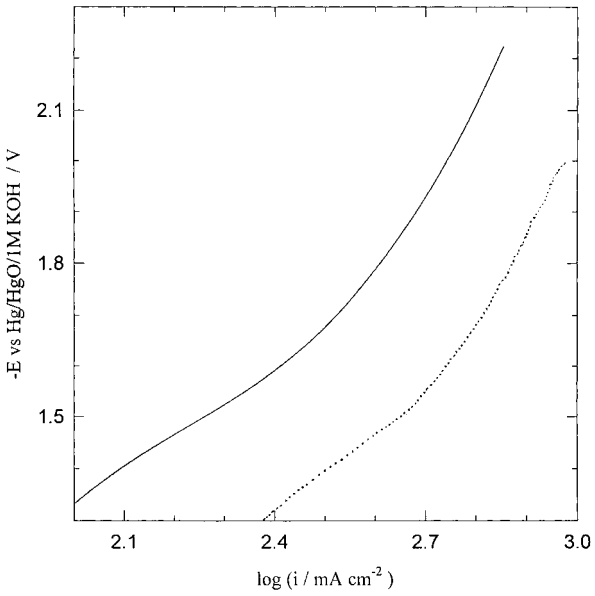

Fig. 6. Comparison between the current-potential relations for h.e.r. on Fe screens and Fe screens/PPy in 1 M KOH at 30 °C and at flow rate of 1.0 cm s^{-1}. Key: (——) Fe screens and (· · · · · ·) Fe screens/PPy.

the cathode. The energy saving in watt hours, $\Delta\xi$ at the cathode at a particular current, i is given by

$$\Delta\xi = \frac{i\Delta E t}{3600} \quad (1)$$

where t is the electrolysis time in seconds, ΔE is the decrease in cathodic potential at a particular current, i, at the cathode brought by the polypyrrole. The values of ΔE were calculated from Figure 6 by subtracting the potentials for Fe screens and Fe screens/PPy at certain current densities. The energy saving, P at the cathode in kWh per kilogram of hydrogen gas is given by

$$P = \frac{i\Delta E(t/3600)}{i(t/F)} = \frac{\Delta E F}{3600} \quad (2)$$

The values of ΔE were calculated at various current densities from data in Figure 6 and plotted against current density as shown in Figure 7. The energy saving per kilogram of hydrogen gas increases with the increase in operating current. The most beneficial effect of the polypyrrole coating appears at an operating current higher than about 370 mA cm^{-2}. This range is of practical interest for water electrolysis.

4. Summary

Polypyrrole film showed good electrocatalytic properties towards h.e.r. from alkaline medium. In general the performance of the Fe/PPy electrode is better than both Fe and Ni electrodes. SEM micrographs confirmed the good adhesion of the polypyrrole film to the iron substrate after relatively long period of h.e.r. at −1.7 V.

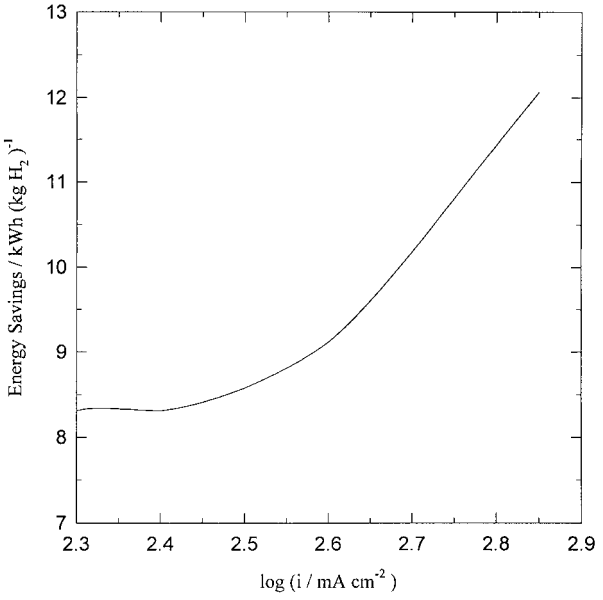

Fig. 7. Relation between the rate of power savings at the cathode as using Fe screens/PPy electrode.

The Fe/PPy film showed good performance and stability at relatively high temperature of about 70 °C. The effect of polypyrrole coating on iron screens was also tested. The PPy coating on the iron screens decreased the potential required to sustain a specific rate of hydrogen production and, hence, the energy consumed during water electrolysis. Finally, it would be of interest to compare the Fe/PPy with roughened Fe and Ni or with Ni/S electrode surfaces.

References

1. B.V. Tilak, B.P.W.T. Lu, J.E. Coleman and S. Sriniavasan, *in* 'Comprehensive Treatise of Electrochemistry', Vol. 2, edited by J.O'M. Bockris, B.E. Conway, E. Yeager and R.E. White (Plenum Press, 1981).
2. D. Plectcher, 'Industrial Electrochemistry' (Chapman & Hall, New York, 1982), Chapter 5.
3. A.J. Appleby and G. Crepy, *in* 'Advanced Electrolysis in Alkaline solution', Proceedings of the Symposium on 'Electrode Materials and Processes for Energy Conversion and Storage', Vol. 77b, edited by J.D.E. Molntyre and S. Srinivasan, (1977), Chapter 4.
4. L. Chen and A. Lasia, *J. Electrochem. Soc.* **139** (1992) 1058.
5. G.P. Kittlesen, H.S. White and M.S. Wrighton, *J. Am. Chem. Soc.* **106** (1984) 7389.
6. M.T. Nguyen and L.H. Dao, *J. Electrochem. Soc.* **136** (1989) 2131.
7. T. Boinowitz, G.T. Suden, U. Tormin, H. Krohn and F. Beck, *J. Power Sources* **56** (1995) 179.
8. T. Shimidzu, A. Ohtani and K. Honda, *J. Electroanal. Chem.* **251** (1988) 323.
9. F. Mizutani and M. Asia, *Bull. Chem. Soc. Jpn* **61** (1988) 4458.
10. M. Umana and J. Walker, *Anal. Chem.* **58** (1986) 2979.
11. S. Holdcroft and B.L. Funt, *J. Electroanal. Chem.* **240** (1988) 89.
12. L.F. Warren, D.P. Anderson, *J. Electrochem. Soc.* **134** (1987) 101.
13. F.T.A. Volk, B.C. Schuemans and E. Barendrecht, *Electrochim. Acta* **35** (1990) 567.
14. A.F. Diaz, J.I. Casillo, J.A. Logan and W.Y. Lee, *J. Electroanal. Chem.* **129** (1981) 115.
15. J.M. Ko, H.W. Rhee, S.M. Park and C.Y. Kim, *J. Electrochem. Soc.* **137** (1990) 905.
16. A. Dall'Olio, Y. Dascola, V. Varacca and V. Bocchi, *C. R. Acad. Sci. Ser. C.* **267** (1968) 433.
17. M. Satoh, K. Imanishi and K. Yoshino, *J. Electroanal. Chem.* **317** (1991) 139.
18. X.Y. Zheng, Y.Z. Ding and L.A. Bottomley, *J. Electrochem. Soc.* **142** (1995) L 226.
19. J.B. Schlenoff and H. Xu, *J. Electrochem. Soc.* **139** (1992) 2397.
20. P. Husler and F. Beck, *J. Electrochem. Soc.* **137** (1990) 2067.
21. M. Schirmeisen and F. Beck, *J. Appl. Electrochem.* **19** (1989) 401.
22. F. Beck and P. Husler, *J. Electroanal. Chem.* **280** (1990) 159.
23. K.M. Cheung, D. Bloor and G.C. Stevens, *Polymer* **29** (1988) 1709.
24. C.A. Ferreira, S. Aeiyach, J.J. Aaron and P.C. Lacaze, *Electrochim. Acta* **41** (1996) 1801 and references therein.
25. J. Newman and W. Tiedman, 'Advances in Electrochemistry and Electrochemical Engineering', Vol. 11, edited by H. Gerischer and C.W. Tobias (Wiley, New York, 1978), p. 352.
26. F. Goodridge and A.R. Wright, *in* 'Comprehensive Treatise of Electrochemistry', Vol. 6, Electrochemical Processing, edited by J. O'M. Bockris, B.E. Conway, E. Yeager and R.E. White, (Plenum Press, New York, 1984), Chapter-6, p. 293.
27. B.G. Ateya and E.S. Arafat, *J. Electrochem. Soc.* **130** (1983) 380.
28. B.E. El-Anadouli, M.M. Khader, M.M. Saleh and B.G. Ateya, *Electrochim. Acta* **36** (1991) 1899.
29. F.A. Vork and E. Barendrecht, *Electrochim. Acta* **35** (1990) 135.

30. M.S. El-Deab, M.E. El-Shakre, B.E. El-Anadouli and B.G. Ateya, *Int. J. Hydrogen Energy* **21** (1996) 273.
31. D. Dobos, 'Electrochemical Data', (Elsevier Scientific, Amsterdam, 1975) pp. 242–267.
32. J.O'M. Bockris and B.O. Yang, *J. Electrochem. Soc.* **138** (1991) 2237.
33. A.J. Appleby, M. Chelma, H. Kita and G. Bronoel, 'Encyclopedia of the Electrochemistry of Elements', edited by A.J. Bard (Marcel Dekker, New York, 1982).
34. T.S. Lee, *J. Electrochem. Soc.* **118** (1971) 1278.
35. M.M. Saleh, John W. Weidner, B.E. El-Anadouli and Badr G. Ateya, *J. Electrochem. Soc.* **142** (1995) 4122.